Supplementary material:

Soil acidity neutralization and clay mineralogy modifications following limestone and dolomitic-limestone application in south Brazil.

Ca saturation and EG solvation of the 0.05-0.1 µm fraction

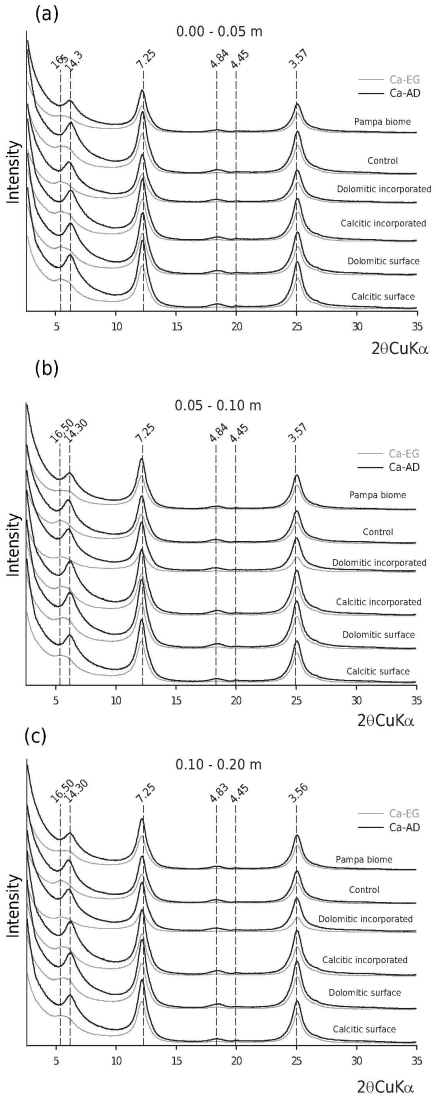


Figure Supplementary Material 1: X-Ray diffraction patterns of the of the 0.05-0.1 µm fraction saturated with Ca in air-dried (CaAD) and solvated with ethylene glycol (CaEG) for the three soil layers. (a) 0.00-0.05 m, (b) 0.05-0.10 m, (c) 0.10-0.20 m

Potassium saturation and heating treatments of the 0.1-2 µm fraction

Samples from the 0.1-2 µm fraction were saturated with potassium and analyzed by X-ray diffraction at room temperature and following thermal treatments at 110°C, 350°C and 550°C

(Figures supplementary material 2 to 4). Although the overall trend was consistent across samples, the intensity of the observed changes varied. At room temperature, potassium saturation induced a partial collapse and splitting of the basal reflection near 14.2 Å. This resulted in two distinct contributions: one peak partially collapsed to approximately 10–10.5 Å, while the other remained near its original position at ~14 Å. Upon heating to 110°C, 350°C, and 550°C, the ~14 Å peak shifted to higher diffraction angles (indicating a decrease in d-spacing), became broader, and lost intensity. Concurrently, the ~10 Å peak exhibited increased asymmetry toward lower angles and gained intensity. The extent of peak shifts and collapse intensity depended on both the thermal treatment and the sampling depth.

For the sample from the 0.00–0.05 m layer of the Pampa biome, potassium saturation at room temperature induced a slight collapse of the peak at ~14.2 Å. Heating to 150°C and 350°C caused the peak to shift to ~13.4 Å and ~13.6 Å, respectively, accompanied by increased asymmetry in the ~10 Å peak. After heating to 550°C, the main peak shifted to ~11.2 Å, while the ~10 Å peak remained asymmetric. The 0.05–0.10 m and 0.10–0.20 m layers exhibited similar behavior, though with a less pronounced collapse at 550°C.

In the control sample, heating to 150°C and 350°C led to a partial collapse of the ~14.2 Å peak, shifting it to between ~13.4 Å and ~11.65 Å. After heating to 550°C, the diffraction pattern showed a band at ~11.65 Å and an asymmetric peak at ~10 Å.

For the 0.00–0.05 m layer treated with surface-applied limestone, potassium saturation induced partial collapse of the ~14.2 Å peak and increased intensity of the ~10 Å peak. Heating to 150°C and 350°C shifted the peak to ~12 Å and ~11 Å, respectively. At 550°C, the peak remained near ~11 Å, while the ~10 Å peak became more intense and asymmetric. The 0.05–0.10 m and 0.10–0.20 m layers showed similar trends, though with reduced peak collapse.

In the 0.00–0.05 m layer treated with surface-applied dolomitic limestone, potassium saturation also caused partial collapse. Heating to 150°C and 350°C shifted the peak to ~13 Å and ~11–12 Å, respectively, with increased intensity of the ~10 Å peak. At 550°C, the peak was observed at ~10.7 Å, and the ~10 Å peak became more intense. The collapse was slightly greater than that observed in soils treated with calcitic limestone. The 0.05–0.10 m and 0.10–0.20 m layers followed a similar pattern, with less pronounced collapse.

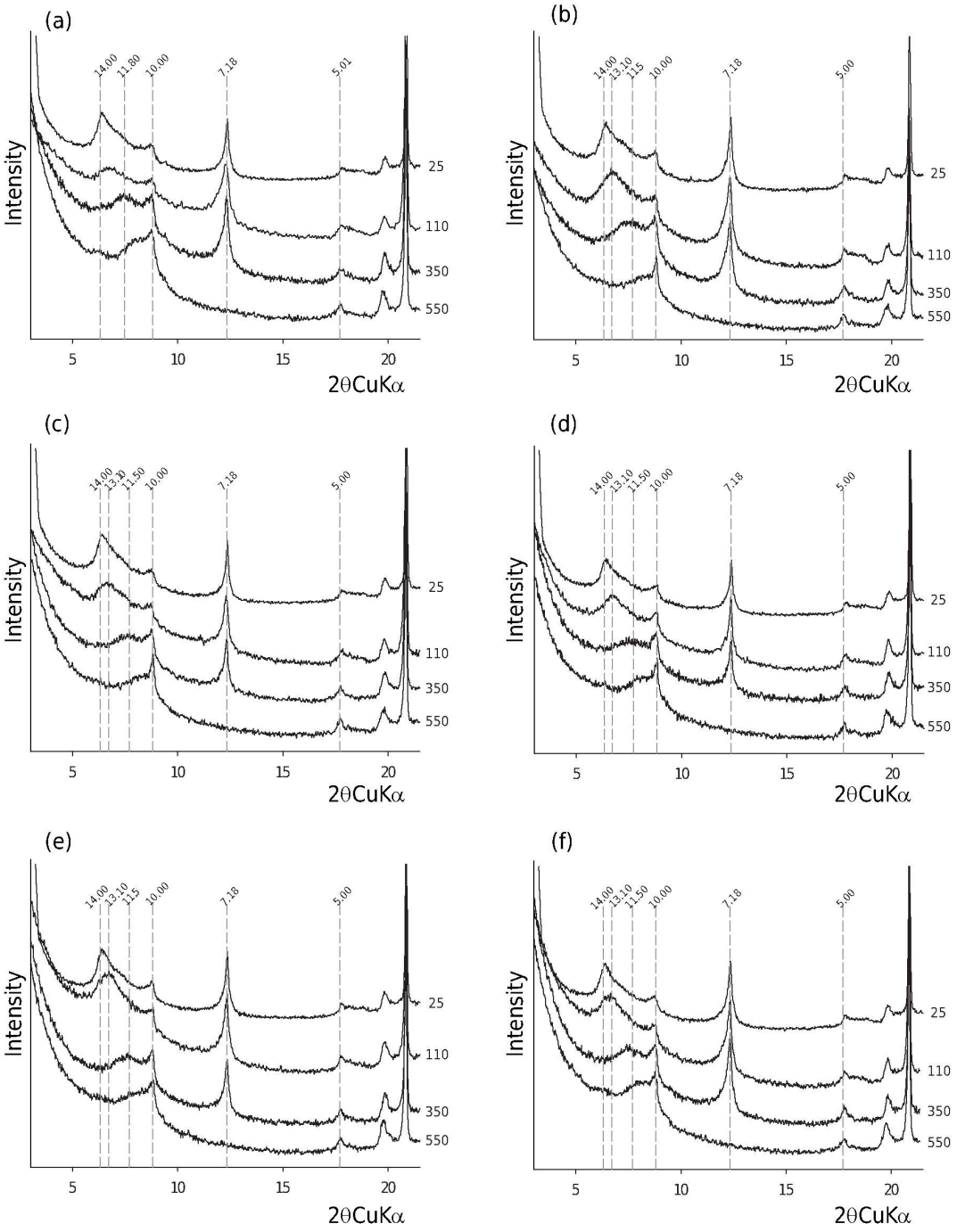


Figure Supplementary Material 2: X-Ray diffractograms of the of the 0.1-2 µm fraction saturated with K in air-dried state (K25) and heated at 110°C, 330°C and 550°C for the layer 0.00-0.05 m. (a) calcitic surface, (b) dolomitic surface, (c) calcitic incorporated, (d) dolomitic incorporated, (e) control (f) Pampa biome

For the 0.05–0.10 m and 0.10–0.20 m layers with incorporated calcitic or dolomitic limestone, greater peak displacement to higher angles (i.e., lower d-spacing) and more pronounced layer collapse were observed. This effect was slightly more significant with dolomitic limestone.

Across all samples, heating to 550°C resulted in the disappearance of kaolinite peaks. Additionally, the 0.1–2 μm sub-fraction contained nearly all the quartz and feldspars present in the bulk clay fraction.

The combination of AD, EG, and K-saturated samples subjected to thermal treatments enables more accurate identification of 2:1 clay minerals. The samples contain a low proportion of illite interstratified with swelling layers, such as vermiculite and smectite. Partial swelling of the ~14.2 Å peak in the AD state following EG solvation, along with progressive collapse after K saturation and heating, indicates the presence of multiple complex 2:1 clay minerals.

Layers that swell partially and collapse upon K saturation at room temperature are attributed to swelling minerals (vermiculite or smectite). Layers that swell in the EG state and collapse to ~10–11 Å upon heating are consistent with hydroxy-interlayered minerals (HIMS) containing both aluminized (non-swelling) and non-aluminized (swelling) layers. Layers that do not swell and collapse directly to ~10–11 Å are also identified as HIMS, but with a higher proportion of aluminized layers and fewer non-aluminized layers, likely with exchangeable Ca^{2+} or Mg^{2+}.

These observations suggest the presence of multiple HIMS populations with varying degrees of layer aluminization, as described by Bertolazi et al. (2017). Differences among samples reflect variations in the relative proportions of these layer types. Overall, limestone-treated soils exhibit a greater swelling capacity and more pronounced collapse following K saturation and heating, indicating a higher proportion of swelling layers compared to control and native pasture samples. Nonetheless, the dominant contribution remains from non-swelling HIMS, suggesting strong aluminization and a limited but detectable impact of limestone application on clay mineralogy.

This behavior is more evident in the coarse sub-fraction, while in the finer fraction, low crystallinity and extensive interstratification mask these effects. Diffraction bands become broader, especially under EG treatment, making interpretation more challenging. Changes in clay mineralogy are inherently difficult to detect in these Ultisols (*Argissolo Vermelho-amarelo distrófico*, which are dominated by kaolinite and contain only minor amounts of 2:1 clay minerals. However, infra-micrometric fractionation reveals that these 2:1 minerals, despite their low abundance, exhibit complex behavior due to varying degrees of aluminization (highlighted by K saturation). This underscores the reactivity of the fine clay fraction in subtropical soils and the critical role even small quantities of 2:1 minerals play in acidity neutralization and cation nutrient retention.

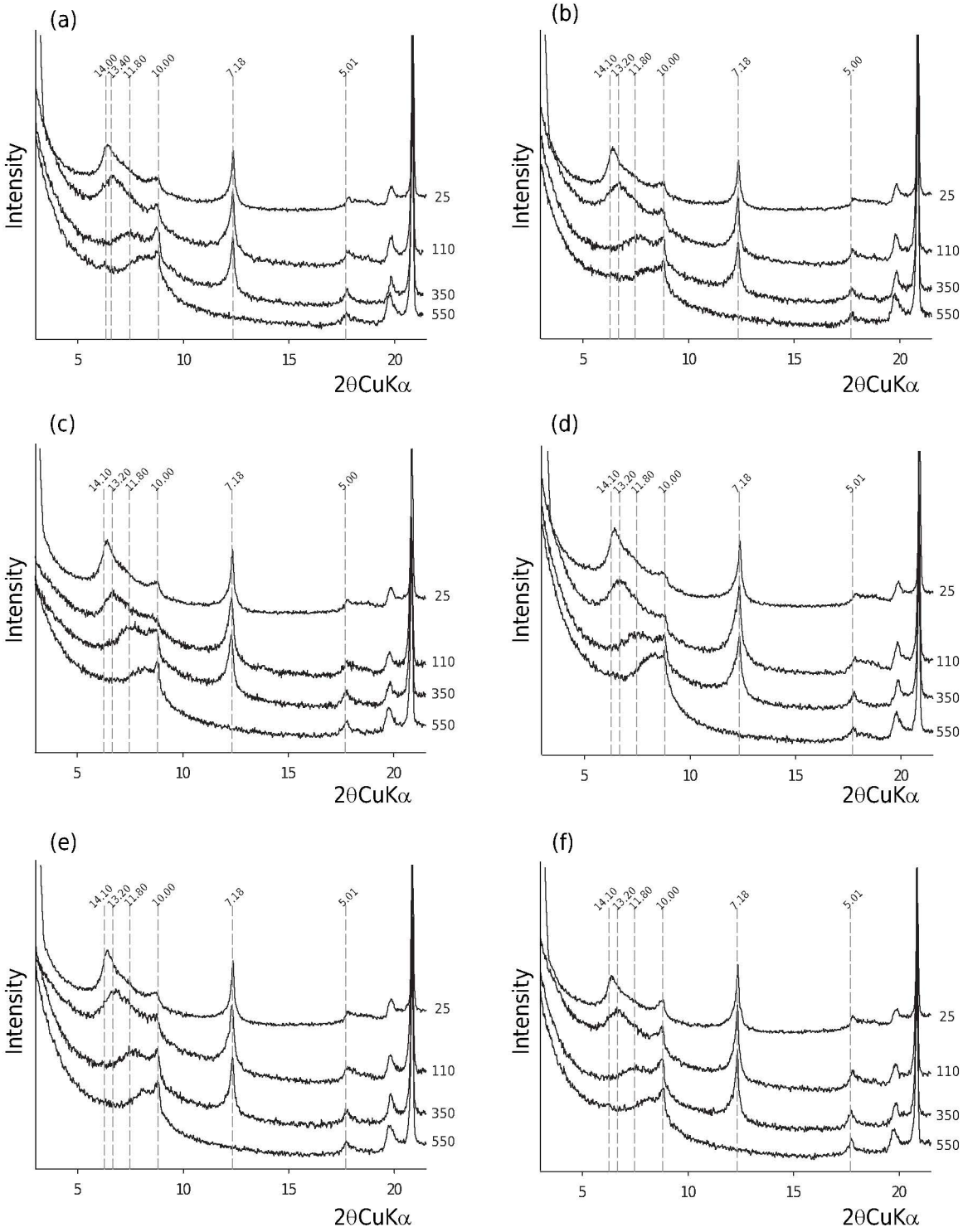


Figure Supplementary Information 3: Xray diffractograms of the of the 0.1-2 µm fraction saturated with K in air-dried state (K25) and heated at 110°C, 330°C and 550°C for the layer 5-10 cm. (A) calcitic surface, (B) dolomitic surface, (C) calcitic incorporated, (D) dolomitic incorporated, (E) control (F) Pampa biome

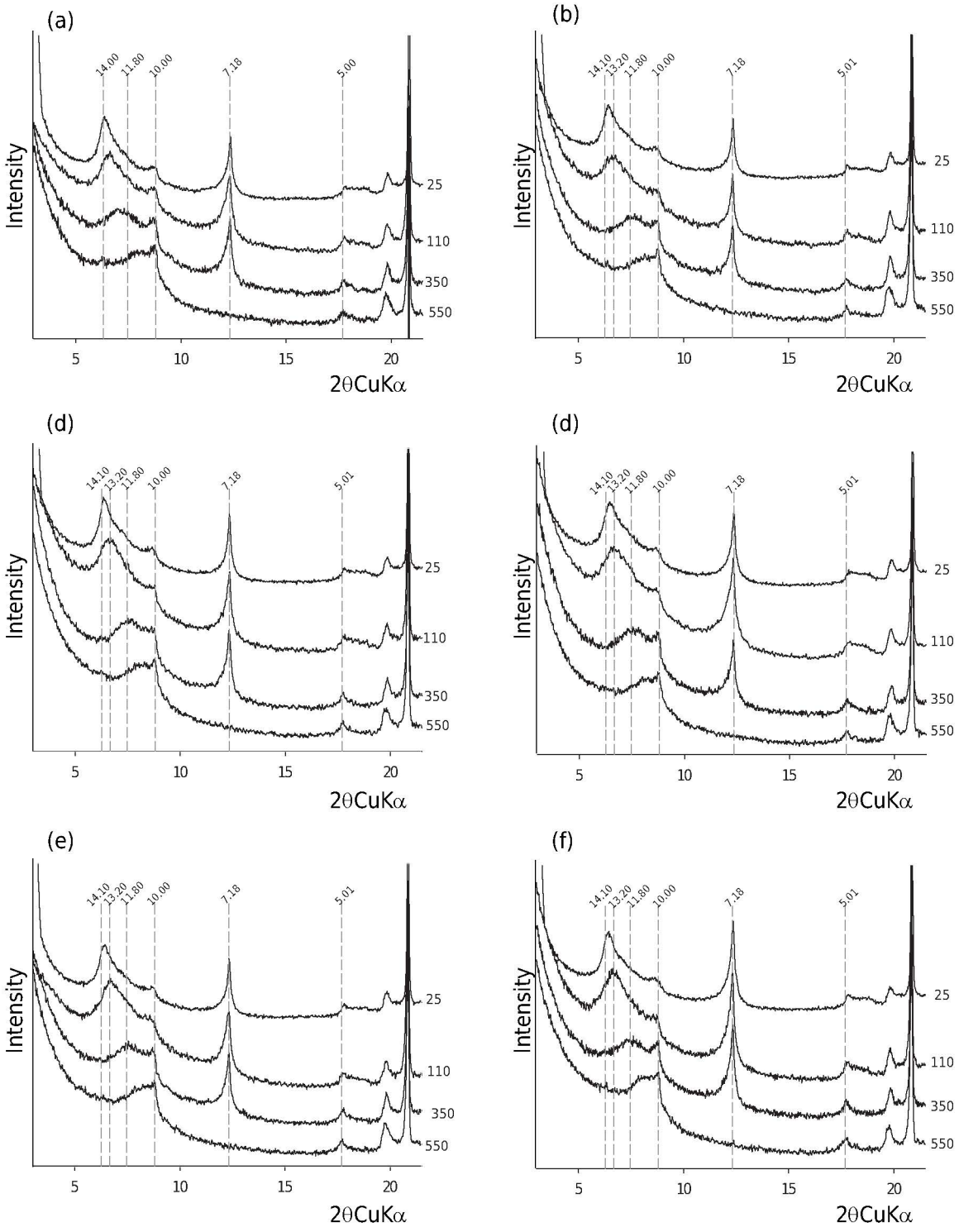


Figure Supplementary Information 4: Xray diffractograms of the of the 0.1-2 µm fraction saturated with K in air-dried state (K25) and heated at 110°C, 330°C and 550°C for the layers 10-20 cm. (A) calcitic surface, (B) dolomitic surface, (C) calcitic incorporated, (D) dolomitic incorporated, (E) control (F) Pampa biome

Exchangeable cations and effective CEC ($cmol_c\ kg^{-1}$) and ratio Ca:Mg.

Exchangeable Ca						
Depth	Calcitic incorporated	Calcitic surface	Dolomitic incorporated	Dolomitic surface	Control	Pampa biome
m	---------- $cmol_c\ kg^{-1}$ ----------					
0.00 – 0.05	5.06	5.26	4.2	4.54	1.79	1.5
0.05 – 0.10	4.04	4.46	3.17	2.42	1.11	0.6
0.10 – 0.20	3.52	3.91	2.31	1.34	0.87	0.4
0.20 – 0.40	3.57	3.12	1.43	1.26	0.94	0.4
Exchangeable Mg						
0.00 – 0.05	1.58	1.51	1.92	2.2	0.93	1.1
0.05 – 0.10	1.4	1.29	1.88	1.91	0.8	0.9
0.10 – 0.20	1.25	1.09	1.37	1.15	0.64	0.7
0.20 – 0.40	0.92	0.98	0.9	0.7	0.44	0.7
Exchangeable K						
0.00 – 0.05	0.23	0.27	0.32	0.23	0.29	0.18
0.05 – 0.10	0.12	0.14	0.18	0.12	0.14	0.1
0.10 – 0.20	0.11	0.09	0.15	0.1	0.11	0.06
0.20 – 0.40	0.09	0.07	0.13	0.09	0.1	0.06
Exchangeable Al						
0.00 – 0.05	0.26	0.04	0.18	0.05	0.74	0.83
0.5 – 0.10	0.41	0.05	0.33	0.19	1.03	0.96
0.10 – 0.20	0.6	0.13	0.52	0.57	1.07	1.28
0.20 – 0.40	0.91	0.59	0.88	0.88	1.11	1.46
CEC*ef*						
0.00 – 0.05	7.13	7.08	6.62	7.02	3.75	3.61
0.05 – 0.10	5.97	5.94	5.56	4.64	3.08	2.56
0.10 – 0.20	5.48	5.22	4.35	3.16	2.69	2.44
0.20 – 0.40	5.49	4.76	3.34	2.93	2.59	2.62
Ca:Mg ratio	---------- unitless ----------					
0.00 – 0.05	3.20	3.48	2.19	2.06	1.92	1.36
0.05 – 0.10	2.89	3.46	1.69	1.27	1.39	0.67
0.10 – 0.20	2.82	3.59	1.69	1.17	1.36	0.57
0.20 – 0.40	3.88	3.18	1.59	1.80	2.14	0.57